

# The final optical identification content of the Einstein deep x-ray field in Pavo

I. John Danziger<sup>1,2</sup> and Roberto Gilmozzi<sup>2</sup>

<sup>1</sup> Osservatorio Astronomico di Trieste, Via G. B. Tiepolo 11, I-34131 Trieste, Italy

<sup>2</sup> European Southern Observatory, Karl-Schwarzschild-Str 2, D-85748 Garching, Germany

Received 13 October 1995 / Accepted 13 December 1996

**Abstract.** The optical identification of all sources revealed in the final analysis of the Einstein deep field observations in Pavo has been completed to the viable limits accessible to spectroscopy. This work combined with previously published data results in the identification of 16 AGN's with the real possibility of 3 further such identifications, while a further 2 probably are spurious. Another AGN is identified in an IPC exposure just outside the boundary of the four HRI exposures. One elliptical galaxy (or cluster) and one dMe star complete the tally. In a  $\log N - \log S$  plot the point represented by these 16–19 AGN's falls precisely on the extension of the line defined by the EMSS data, and somewhat below the line defined by the more recent deep field ROSAT data. It extends to fainter sensitivities than the previously published work from the Einstein observations of the same field. It is consistent with the more recently published data for Pavo obtained with ROSAT even though this latter reaches a slightly fainter sensitivity. This identification work therefore sets a firm lower limit to the AGN content of the X-ray identifications in Pavo.

By virtue of having selected in this survey intrinsically fainter-than-average AGN's it has been possible to show, by combination with data for higher luminosity quasars, that a correlation exists between the luminosities and (B–V) colours extending over a luminosity range of 6 magnitudes. This sequence coincides with the sequence obtained by plotting data for all AGN's in the same redshift range taken from the Véron and Véron catalogue. It is argued that the magnitude of this effect cannot be explained by the translation of various strong emission lines through the band-passes of the relevant filters. It may be explained by the influence of host galaxies.

**Key words:** galaxies: active – quasars: general – galaxies: Seyfert – X-rays: galaxies

---

## 1. Introduction

The main purpose of the Einstein Observatory deep X-ray surveys was to define and identify the discrete source contribution

to the isotropic X-ray background down to the sensitivity limit imposed by those observations ( $\sim 2 \times 10^{-14}$  ergs  $\text{cm}^{-2}$   $\text{s}^{-1}$  in the 0.8–3.5 keV energy range). Because of the known X-ray characteristics of AGN's (quasars and active galactic nuclei) and their increasingly accurate optical number counts down to magnitudes  $B < 21.0$  it was clear at the start of this optical identification project (see Giacconi and Zamorani 1987 and references therein) that the proportion of AGN's in the identified source content of these X-ray surveys was significant, if not dominant as suggested by Setti and Woltjer (1982). Thus optical identification provided a clear way to test competing cosmological ideas within which framework one might hope to identify new classes of X-ray objects if they exist at larger redshifts.

A first attempt to optically identify Einstein Observatory sources in the Draco and Eridanus fields by Giacconi et al. (1979) revealed only 2 AGN's in each field out of a combined total of 43 detected X-ray sources. Only in the case of Eridanus has further identification of extragalactic sources proved fruitful, since to date Gilmozzi and Danziger (work in progress) have identified 4 more AGN's and 2 galaxies. The Pavo field ( $40 \times 40$  arcminutes) has proven more rewarding (Griffiths et al. 1983). Of the 17 original X-ray sources discussed by these authors (16 HRI and 1 IPC) 4 were spectroscopically identified with AGN's and one with either an E galaxy or cluster of galaxies. Subsequent spectroscopic work by Griffiths et al. (1992) identified from the original list of 17 sources 7 AGN's, of which 4, because of poor signal/noise, were considered uncertain either with respect to redshift or type.

In the meantime a new analysis of the same Einstein HRI and IPC exposures on Pavo has become available (Primini, private communication). This finds 15 of the 17 original sources but fails to detect 2 of them. However down to a confidence level of  $3.5 \sigma$  another 6 HRI sources and 1 IPC source have been detected. Another 3 with confidence level less than  $3.5 \sigma$  and detected only in the largest analyzing box have been rejected at the outset.

The results of this paper discuss the optical spectroscopic identification of all sources originating from the two analyses mentioned above. We believe that this work completes all identi-

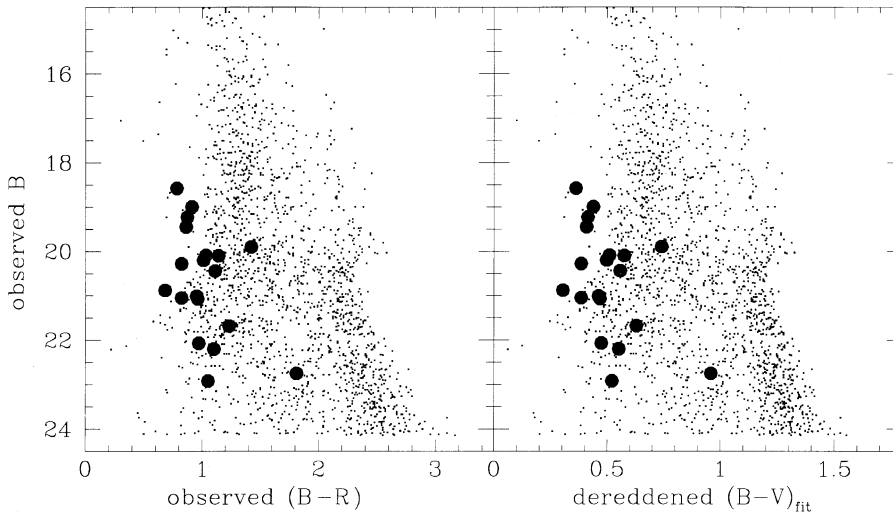


**Fig. 1.** *Left:* The HR diagram (B vs. B-R) derived for stellar-like objects in the Pavo field. Large filled circles represent the optically identified X-ray sources. The magnitudes are COSMOS photographic magnitudes calibrated with CCD data. *Right:* The HR diagram (B vs. B-V) for the same objects using the transformation and reddening correction described in the text.

fications that are feasible with currently available ground-based telescopes.

This work on the Pavo field can provide confidence that the nature of the sources at  $z \sim 1$  and their evolution have not dramatically changed from that predicted on the basis of what is observed at lower redshifts (Setti 1992). This would require the source content to consist predominantly of AGN's with evolution similar to that observed for optically selected AGN's.

## 2. Observations

The program of optical spectroscopic identification of sources arising from the 2 analyses of the Einstein Observatory observations mentioned above has been conducted almost entirely with EFOSC1, the faint object spectrograph and camera, mounted at the Cassegrain focus of the 3.6 m telescope at ESO, La Silla. All of the spectra have a resolution of approximately  $18 \text{ \AA}$  and cover a range of  $3700\text{--}7000 \text{ \AA}$ . They have been flux calibrated through the observation of Oke (1974) white dwarf standards on the same night.

The identification of the most probable candidates in the X-ray error boxes has been considerably assisted by using the same J and F emulsion plates referred to in Griffiths et al. (1983), but by also involving a conversion to photometric B, R magnitudes through CCD imaging of selected fields within the boundaries of the original plates. This colour magnitude diagram (B, B-R) is shown in Fig. 1a, where the shape of the general distribution of objects may be contrasted with that apparent in the original (J, J-F) diagram, where a skewness introduced by the inadequately calibrated photographic photometry could have been noted. The positions of the finally established optical identifications are marked in this figure, where it can be seen that the AGN's, as expected, occupy a small range in colour. The B, R magnitudes for the identified sources are presented in Table 1. Also presented in Table 1 are the astrometrically determined positions of the optically identified sources using the plate scanned by COSMOS and the Guide Star Catalogue. Additional entries

include the difference between the optical and X-ray positions, the HRI fluxes or in one case the IPC flux, the optical identification and the redshift  $z$ . The error boxes associated with the X-ray positions are in the range 5–10 arcseconds.

Finding charts for the 7 new sources discussed below are given in Fig. 2. The reader is referred to Griffiths et al. (1983) for the first 17 sources.

The flux calibrated spectra of all identified sources obtained in this programme are displayed in Fig. 3. We have not obtained new spectra of #5, #7 and #11 since those identifications and redshifts were considered beyond doubt. The decrease in the UV continuum of Pavo #9 and #10 is almost certainly due to atmospheric dispersion effects resulting from observation at large zenith distances.

In the following discussion and in Table 1 we have classified the optical identifications in the following way. If the objects were unresolved and have broad emission lines they have been classified as QSO's. If they are resolved and have narrow lines, they are classified as Seyfert 2 if any line ratios are consistent with this classification. Both categories are considered AGN's.

Some of the proposed identifications merit detailed comment.

Pavo #2 (3#5) can be considered uncertain as a bona fide X-ray source because it is detected near the edge of one HRI field, but not in the second, where it should be closer to the centre of the field. It has not been detected by ROSAT. The distance, 17 arcseconds, of the proposed emission line galaxy from the centre of the field is somewhat greater than the X-ray average for all sources, but not impossibly so. However X-ray variability of this source could possibly explain the facts reported above. A variation of a factor  $> 3.5$  (not exceptional) in the flux would be implied if variability were the cause. On the basis of the available spectrum we cannot distinguish between a genuine AGN and a star-forming galaxy. Thus this identification is considered possible. Another brighter object slightly closer to the X-ray position is a star, but it is optically too faint to be a viable candidate ( $\log f_x/f_{opt} \sim 0.2$ , well above the range observed in stars).

**Table 1.** X-ray sources in Pavo

Orig. Einstein No.	New Einstein No.	RA optical, J2000.0	Dec	Separation X-ray – opt (arcsec)	HRI flux 0.2–3.5 keV ( $10^{-14}$ erg s $^{-1}$ cm $^{-2}$ )	Optical ID	z	B	R
1	2#6	21 12 13.67	–67 49 34.0	2.5	5.6±2.0	QSO	1.002	20.5	19.3
2	3#5	21 12 55.80	–67 53 13.6	17.0	7.4±2.0	E.L. Gal	0.396	21.7	20.5
3	— <sup>c</sup>	21 12 55.80	–67 38 12.1	7.2	—	YSO		21.1	20.1
4	3#1	21 14 11.80	–67 34 36.9	1.4	3.1±1.3	QSO	0.696	22.1	21.1
5	2#9	21 14 21.48	–68 01 07.0	9.1	8.4±2.0	E GAL	0.13	16.4	13.5
6	2#1	21 14 36.96	–67 48 39.6	4.2	5.6±1.3	YSO faint		22.9	21.9
7	1#2	21 14 51.64	–67 48 55.9	2.9	12.3±2.0	QSO	0.91	20.1	19.1
8	3#2	21 14 55.54	–67 41 58.9	3.0	7.5±1.3	QSO	1.020	21.1	20.1
9	4#5	21 15 11.20	–67 47 49.0	5.6	4.4±1.3	QSO	0.765	21.1	20.2
10	1#1	21 15 40.88	–67 46 20.5	1.1	6.5±1.3	QSO	0.708	20.1	19.0
11	1#7	21 15 44.87	–67 54 03.7	2.9	6.4±1.3	QSO	1.13	19.0	18.1
12	4#1	21 15 56.63	–67 35 21.7	1.1	23.2±2.0	QSO	0.549	18.6	17.8
13	1#4	21 15 58.47	–67 51 14.7	1.2	7.4±1.3	Sey 2	0.408	19.8	18.5
14	1#6	21 16 35.85	–67 52 03.1	1.8	7.8±2.0	QSO	0.505	20.3	19.5
15	1#3	21 16 36.78	–67 51 01.9	X-ray <sup>a</sup>	3.6±1.3	empty			
16	—	21 17 44.14	–67 51 59.5	X-ray <sup>a</sup>	—	QSO	0.800	22.2	21.1
17	2#3	21 13 49.23	–67 54 56.1	1.9	3.6±1.3	QSO	0.685	22.8	20.9
	1#5	21 17 15.72	–67 51 49.0	2.2	7.6±2.0	QSO	0.756	20.9	20.2
	1#8	21 16 44.69	–68 05 16.1	5.7	11.3±2.0	QSO	1.229	19.2	18.4
	1#9 <sup>c</sup>	21 14 52.80	–67 54 57.2	(24.8)	4.0±1.3	GAL 20''?	(0.156)	(21.0)	(19.2)
	2#5	21 12 01.48	–67 45 10.7	3.5	7.2±2.0	M4V	0	17.8	15.7
	2#7	21 12 22.68	–67 55 39.7	1.1	5.1±1.3	QSO	1.158	20.2	19.2
	4#8	21 15 07.56	–67 49 35.0	6.9	5.9±2.0	Sey 2	0.126	19.5	18.6
	IPC#1	21 10 09.46	–67 49 15.7	X-ray <sup>a</sup>	22 (IPC)	QSO	0.61	— <sup>b</sup>	— <sup>b</sup>

**Notes:** <sup>a</sup> X-ray means the X-ray position is given because an optical astrometrically determined position is not available

<sup>b</sup> Outside field of original COSMOS plate

<sup>c</sup> Possibly spurious

Pavo #3. It did not appear in the second reduction nor in the ROSAT observations. The YSO measured to have  $B = 21.7$  from the original plates has proven too faint to give a viable spectrum in many hours of integration time. It is probably spurious.

Pavo #6 (2#1) does not have a spectroscopic identification because the yellow stellar object in the error box has proven too faint. The optical colours and the ratio of X-ray to optical luminosity are consistent with its being an AGN and consequently the correct identification. It has also been detected by ROSAT. We consider this identification as an AGN (or conceivably a star-forming galaxy) highly probable.

Pavo #13 (1#4). The optical counterpart is slightly resolved and has narrow emission lines. The strength of [Ne V] 3426 would favour the classification as a Seyfert 2 type galaxy.

Pavo #15 (1#3) has been detected in both analyses of the Einstein data and by ROSAT and therefore is probably not a spurious detection. Nevertheless a candidate optical counterpart is not apparent in the error box. An implied limit to the optical brightness  $> 23.5$  is not inconsistent with its being an AGN but nothing more can be said.

Pavo #16 was not detected in the second analysis of the Einstein observations. It is conceivable that this is because it was towards the edge of the field. While a clear-cut source detection at this position in the ROSAT data is not striking, there is in the harder band image an extension from a softer source to this position. To complicate matters further, the source lies just at the edge of the support structure of the ROSAT camera. The

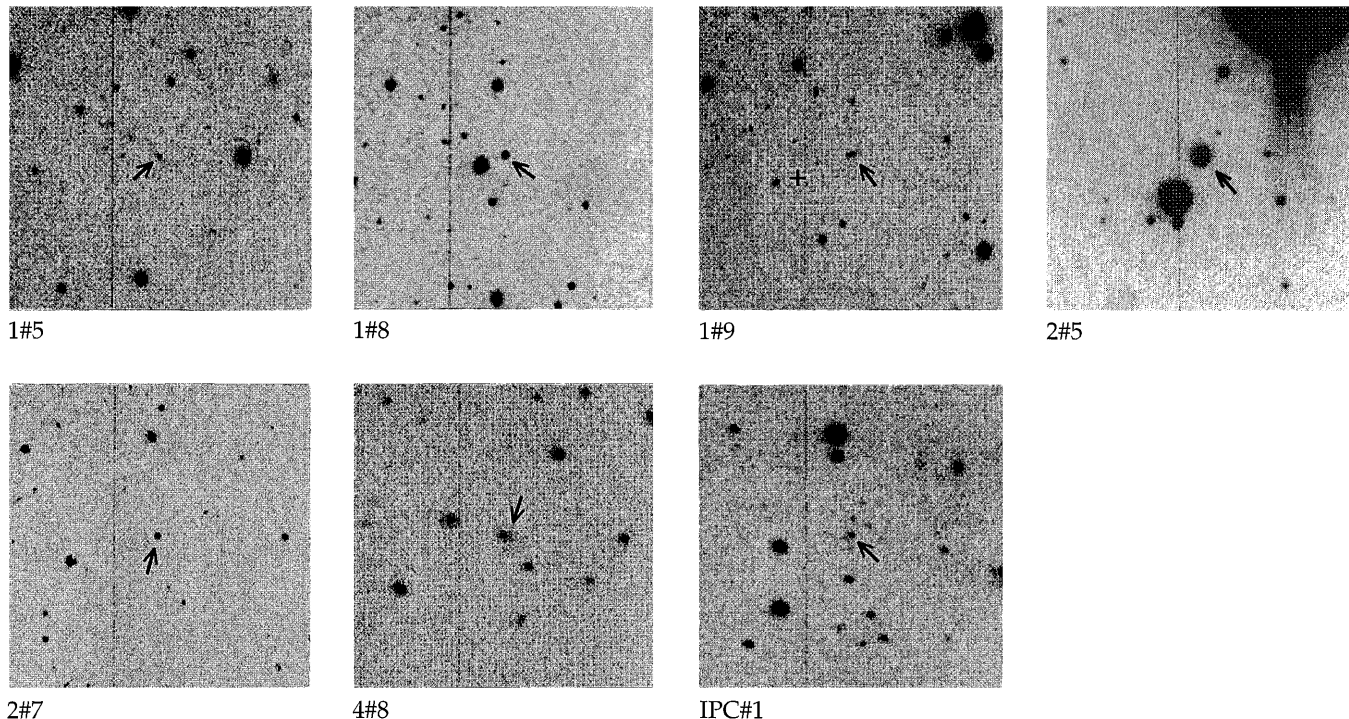


**Fig. 2.** Finding charts for the seven new sources discussed in the text. North is at the top, east to the left. Each chart with a field of 3 arcminutes is centred on the optical counterpart. For 1#9 a cross marks the X-ray position.

low redshift QSO near the X-ray position we consider to be the correct identification.

Pavo 1#9 was not found in the first analysis of the Einstein observations but was detected as a weak source in the second. It has not been detected by ROSAT. The only viable identification is a galaxy 25 arcseconds from the X-ray position. In addition, since this is well beyond the expected error box, we consider that this source may be spurious. There is a star closer to the X-ray position but it is optically too faint to be a viable candidate ( $\log f_x/f_{opt} \sim 0.4$ ).

Pavo 2#5 was not found in the first analysis of Einstein data but appeared in the second, and has been detected by ROSAT. The proposed identification with a dwarf Me star is not contradicted by the X-ray/optical luminosity ratio ( $\log f_x/f_{opt} \sim -1$ ) which is well within the typical range for M stars. A second much fainter star ( $B \sim 23$ ) just outside the X-ray error circle is also an M star, but optically far too faint to be a viable candidate ( $\log f_x/f_{opt}$  would be  $\sim 1$ , almost two orders of magnitude higher than the highest values observed in M stars). It is the only star suggested as an identification for an Einstein X-ray source in Pavo.

Pavo 4#8 was not detected in the first analysis of Einstein observations but appeared in the second. It did not appear in the ROSAT analysis. We believe that the proximity of the identified AGN (6.9 arcsec) to the X-ray position strengthens the case for this being a real X-ray source with an AGN optical counterpart. The optical image is clearly extended. The [O III] 5007/H $\beta$

ratio ( $\sim 5$ ) favours, but not conclusively, the probability that it is a Seyfert 2 galaxy.

IPC #1 was detected in an IPC exposure and identified with a QSO ( $z = 0.61$ ). It is included in Table 1 for the sake of completeness of this project on Einstein Pavo sources. Because it falls just outside the boundary of the four HRI fields, it is not included in the statistical analysis.

Summarizing the optical identifications, we believe that 17 sources (including IPC #1) are almost certainly associated with AGN's while another 3 may have AGN optical counterparts. There is one E galaxy (or cluster) and one dMe star. The remaining 2 lack sufficient information to justify any strong conclusion. A faint AGN origin is not excluded, but neither is the possibility that they are spurious X-ray detections.

### 3. Calibration of HRI counts

In order to translate the HRI rates into the fluxes given in Table 1 we have taken our own experimental approach: we have used the IPC fluxes (0.8–3.5 keV) of objects having both IPC and HRI measurements to determine a conversion factor. In our Pavo sample, there are 7 such objects (all QSOs), which provided a conversion factor of  $4.2 \pm 1.1$  (flux in  $10^{-14}$  erg  $s^{-1} cm^{-2}$ , HRI counts in  $10^{-3}$  cts  $s^{-1}$ ). This factor becomes  $4.0 \pm 1.2$  if each point is weighted by  $1/\sigma$ . To check the validity of this method we have also computed the conversion factor using the data presented by Primini et al. (1991). From their sample we have selected only point sources (we included some

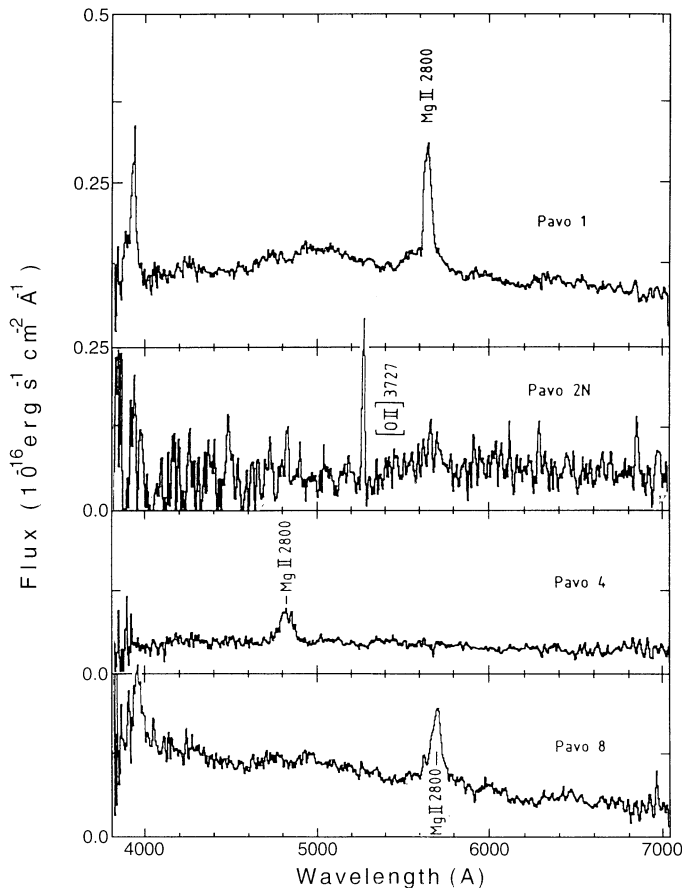


**Fig. 3a.** Flux calibrated spectra for the optical identifications not previously published.

stars as well, since the number of QSOs with both HRI and IPC measurements was small). In some cases, more than one HRI measurement was available (we used the average), and in one case, two HRI sources were present in the same field (we used the HRI counts for the confirmed QSO, the other HRI field being empty). Three of Primini et al.'s sources are in common with our sample (both IPC fluxes and HRI counts agree very well within the uncertainties, though the data reduction used by Primini et al. was a more recent one). The conversion factor from their data is  $4.0 \pm 1.2$  ( $3.5 \pm 1.0$  weighted: the difference is mostly due to the effect of one very bright source, their number 1). Combining all the data (without excluding the 3 sources in common) yields a factor  $4.1 \pm 1.1$  (or  $3.7 \pm 1.0$  weighted). We prefer the combined weighted mean value from our method as a conversion factor.

Fig. 4 shows the combined samples. The fit in the top panel is to the Primini et al. data only. The fact that it fails to go through zero may signify some problems in the background subtraction, or be simply an effect of the different bandpasses for IPC and HRI. The lower panel shows that this, however, is not a serious problem when one deals with ratios. Note that the lower panel is *not* a plot of the residuals of the fit, but just the ratio of IPC fluxes to HRI counts.

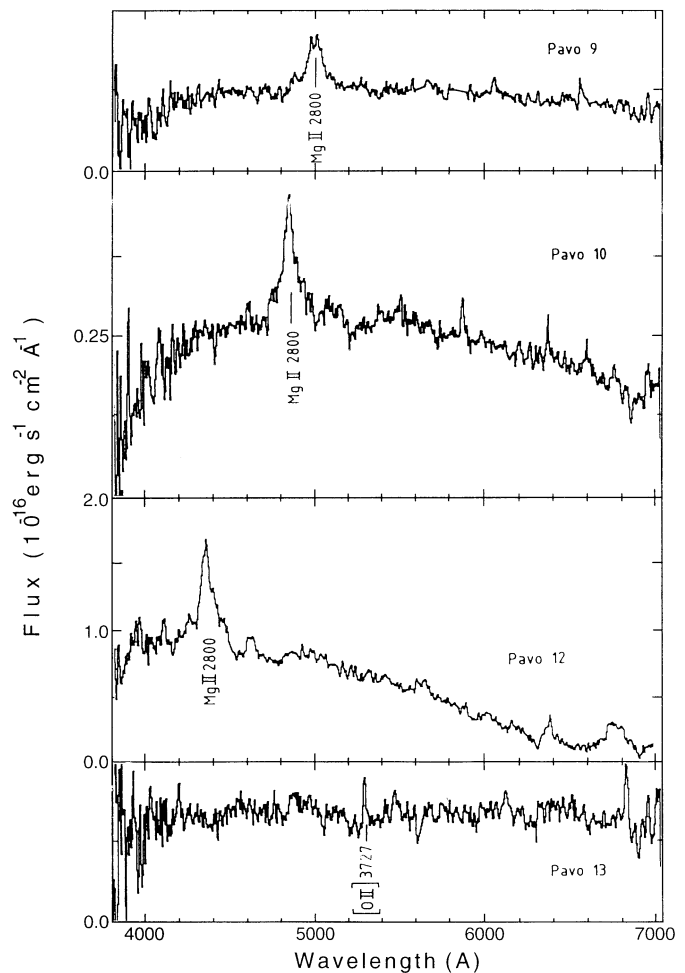


**Fig. 3b.** Flux calibrated spectra for the optical identifications not previously published

This method of calibrating the HRI rates is subject to a criticism that source variability between the times of HRI and IPC observations could invalidate the method. However the consistency of the calibration obtained from 2 different samples provides some reassurance on this point, as does the good agreement with the calibration available from the Einstein Manual.

Our calibration translates to 7.2 in the 0.2–3.5 keV HRI band compared to 6.2 from the Einstein Manual. In the following discussion as well as in Table 1 we adopt a mean value of 6.7 (flux in  $10^{-14}$  ergs  $s^{-1}$   $cm^{-2}$ , HRI counts in  $10^{-3}$  cts  $s^{-1}$ ).

#### 4. Comparison with other source counts

We have shown that in the 40 arcminute square field of the Pavo HRI fields there are 16 virtually certain AGN identifications with the possibility of 3 more AGN source identifications, and with a further 2 X-ray detections either spurious or too weak to be included in our considerations. These numbers do not include one E galaxy (or cluster) and one dMe star.

The 16–19 sources translate into 36–42.8 / square degree. We can plot this point in the log N–log S diagram for the

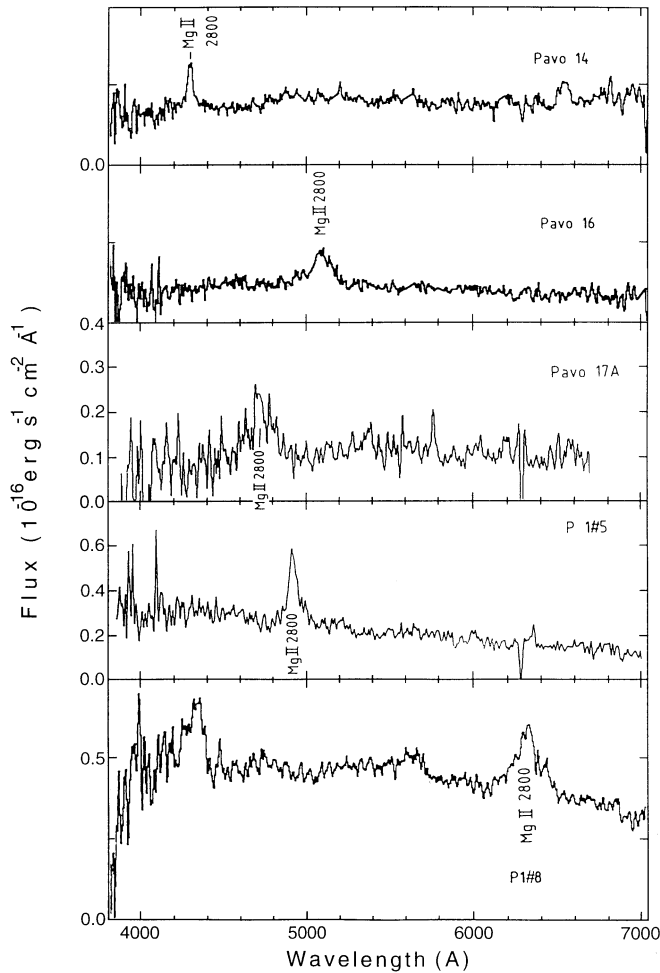


**Fig. 3c.** Flux calibrated spectra for the optical identifications not previously published

0.5–2.0 keV band published for ROSAT data by Hasinger et al. (1993). To do this we have taken the limit of sensitivity to be the HRI count (0.46) for the weakest authentic source and converted to the 0.5–2.0 keV band assuming a spectral index for the sources of  $-1$ . This limit corresponds to  $1.49 \times 10^{-14}$  ergs  $\text{cm}^{-2} \text{sec}^{-1}$ .

The following points may be noted. This work extends the previous work on the Einstein Pavo field (Primini et al. 1991) to fainter limits owing to the success in optical identification in HRI fields where some confidence in the flux calibration was established.

As can be seen in Fig. 5, this new point falls almost precisely on the extrapolation of the line for the EMSS data published by Gioia et al. (1990). It falls 30 per cent below the ROSAT deep survey at the same sensitivity in the Lockman Hole published by Hasinger et al. (1993). There could be one or more reasons for this discrepancy. Statistical fluctuations alone may not explain discrepancies of this kind. Other possibilities include incompleteness in our detections, the presence of an undetermined proportion of galactic sources in the ROSAT data, or the existence of significant fluctuations due to large scale structure.

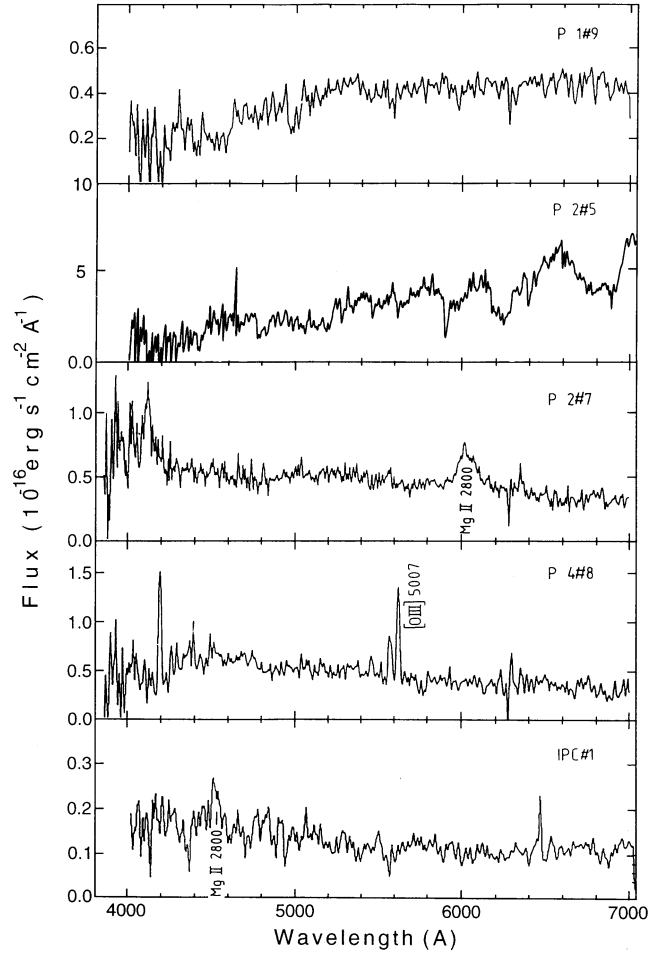


**Fig. 3d.** Flux calibrated spectra for the optical identifications not previously published

A determination of the degree of completeness of our sample with a  $V/V_{max}$  test is impractical because the sample is too small and we do not know a priori the amount of evolution intrinsic to this sample. Large scale fluctuations from one area to another appear to be present as evidenced by the data for the individual deep fields presented by Hasinger et al. (1993). At a given limiting sensitivity factors of 2 or more are apparent in the surface density of X-ray sources. Indeed the ROSAT data for Pavo presented by the above authors falls at least as far below the data for the Lockman Hole as does our Einstein point at slightly lower sensitivity. Nevertheless since our identifications are virtually complete our result provides a firm lower limit to the space density of X-ray selected AGN's in the Pavo field.

The surface density of optically identified quasars begins to exceed our X-ray identified quasars by progressively larger percentages as one proceeds to fainter than B magnitude 21.0 (Cristiani and La Franca 1995; Zitelli et al. 1992). Thus other quasars in the Pavo field brighter than 22.5 B magnitude remain undetected because their X-ray luminosities lie below the Einstein sensitivity limit. The ROSAT observations should uncover most of these.

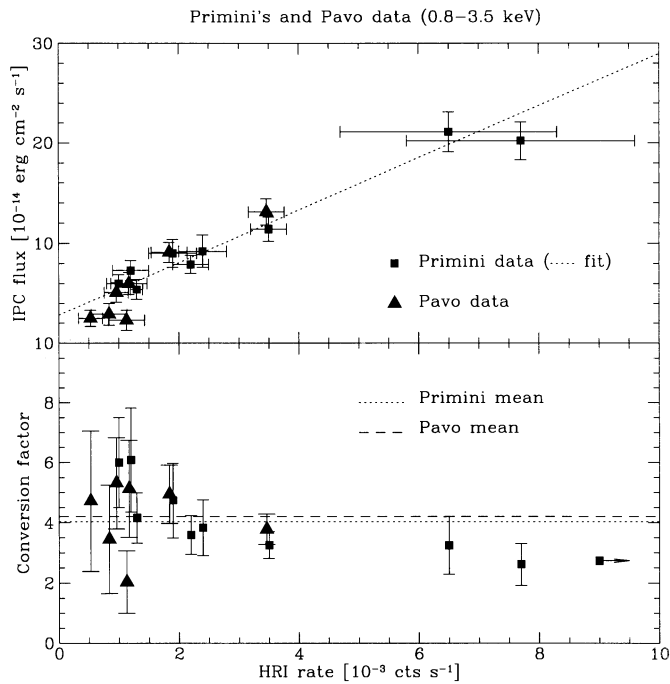


**Fig. 4.** Upper panel. A plot of the observed IPC fluxes versus HRI counts for objects from this sample and from data published by Primini et al. (1991). Lower panel. A plot of the conversion factor for each individual object versus the HRI count.

## 5. The colour-luminosity diagram for quasars

The observed average B–R colour for the Einstein Pavo sources is 0.97, as can be seen in Fig. 1, and corresponds to a reddening corrected B–R = 0.89. The optically selected sample of quasars of Wilkes et al. (1994) has an average B–V  $\sim$  0.3 corresponding to the colour of an FO star for which B–R would be 0.61 in contrast with the value of 0.89 for Pavo AGN’s. However the Wilkes et al. sample in the redshift range  $z = 0.4$ –1.2 has an average B magnitude  $B \sim 18.0$  and cuts off at  $B = 20$ . In contrast our Pavo sample has an average  $B \sim 21.0$ . Therefore in Pavo, by virtue of the X-ray selection, we are sampling lower luminosity AGN’s. A first comparison with the Wilkes et al. sample has been made because although optically selected all are X-ray sources.

In order to compare our data with those of Wilkes et al., we have to perform a conversion from B–R colours to B–V colours. Although such conversion is of course dependent on the details of each spectrum, if one assumes that the colours of the QSOs are not affected significantly by the emission lines (an assumption supported by the spectroscopy), the conversion from B–R to B–V for the QSOs can be obtained by applying the transformation valid for stars of similar colours. This has been determined by fitting a 4th degree polynomial to the intrinsic B–V and B–R colours of main sequence stars (e.g. Johnson 1966) in the range of interest ( $0 < B-R < 3$ ) and applying the fit to the dereddened B–R colours of all the objects of Fig. 1a. The result is shown in Fig. 1b (no reddening correction has been applied to the B magnitude in the figure to avoid mismatching y-axes).

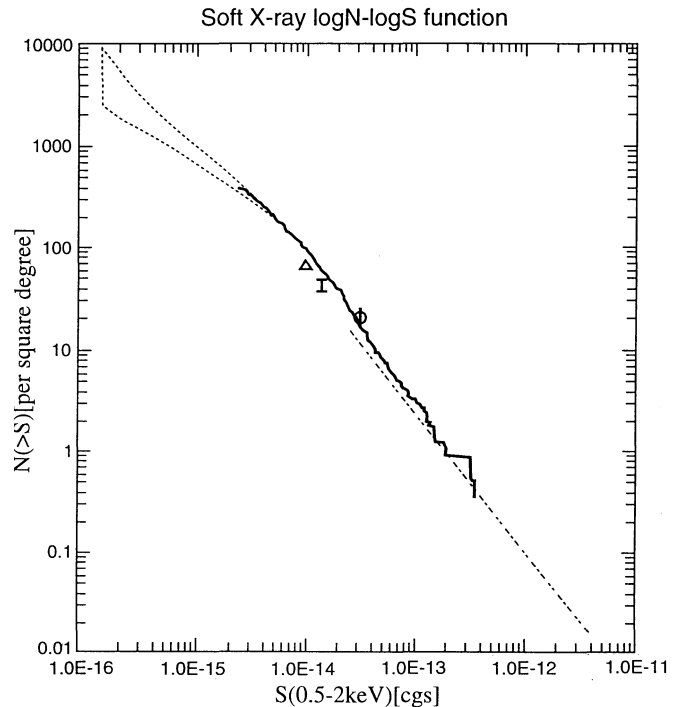


**Fig. 5.** The log N–log S plot for the energy range 0.5–2 keV taken from Hasinger et al. (1993). The open triangle represents the point for the Pavo ROSAT observations given in that paper. The vertical bar with 2 horizontal bars comes from our identification of sources in the Einstein data. The lower horizontal bar represents the minimum number of identified AGNs. The upper bar represents the 19 possible AGNs plus the E galaxy plus the dMe star. The circle with the error bar represents the Einstein extended deep survey point (Primini et al. 1991) scaled by a factor 1.32 to account for stars in the sample (Hasinger et al. 1993).

If we judge that a least-squares fit on the Pavo AGNs alone would give B–R = 1.15 at  $B = 23.0$ , this corresponds to a dereddened B–V = 0.64. This fit falls close to the least-squares fit to the brighter AGN’s in the same range of  $z$  in the sample of Wilkes et al. (1994).

An observed colour-magnitude diagram combining our sample and the Wilkes sample is given in Fig. 6 for all objects in the redshift range 0.4–1.2. Also plotted are observed colours and magnitudes for all AGN’s in the same redshift range taken from the Véron and Véron Catalogue (1996).

In Fig. 6b we plot absolute magnitudes calculated using the data of Fig. 6a, the known redshift and an assumed value of  $H_0 = 75 \text{ km s}^{-1} \text{ Mpc}^{-1}$  and  $q_0 = 0$ . K corrections to the magnitudes as a function of redshift using the published data of Cristiani and Vio (1990) have been included. In this plot we have included all AGN’s with redshift  $< 1.2$  from the Véron and Véron Catalogue. In this way one can see the sequence defined at low luminosities by objects known to be galaxies.

Thus it appears that there is a correlation of luminosity with colour over a range in  $B$  16–23.0 with a slope  $\sim 0.065 \text{ mag}(B-V) / B_{\text{mag}}$ . In order that no correlation would exist the Pavo quasars would also need a  $(B-V) = 0.3$ , and this requires either

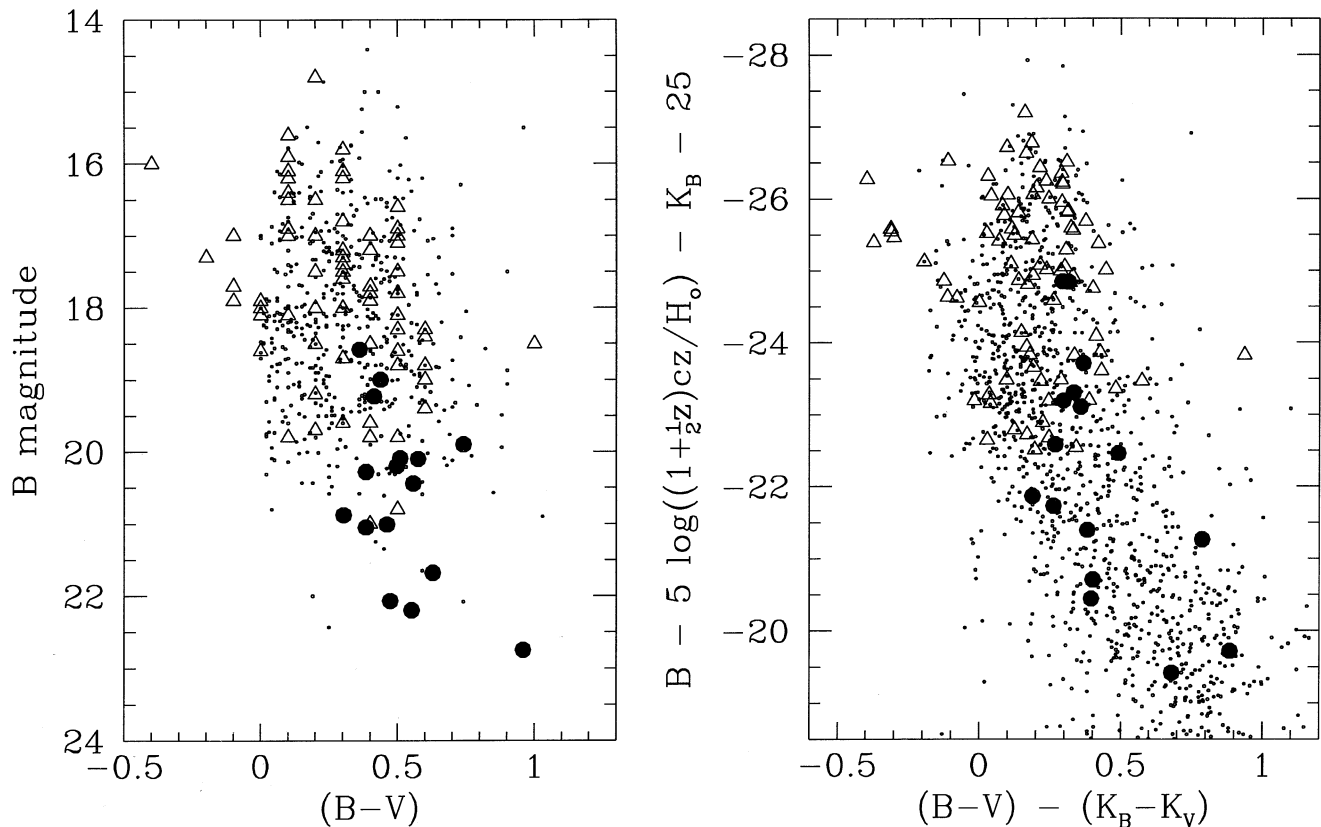


**Fig. 6.** *Left:* The HR diagram constructed from our derived colours for the AGN’s identified in the Pavo field (*filled circles*) together with the data for optically selected quasars presented by Wilkes et al. (1994) (*open triangles*) together with data for AGN’s taken from the Véron and Véron Catalogue (1996). The redshift range  $z$  embraced by this data is 0.4–1.2. *Right:* The colour-magnitude diagram for objects in 6a (see text for assumptions) but also including AGN’s from Véron and Véron with  $z < 0.4$ .

a severe error in the zero point determination of the magnitudes ( $> 0.2$  mag in each filter) or a large effect of emission lines on colours. The first possibility seems to be ruled out by noting that the vertical strip of stars between B 15–21 has a mean  $B-V = 0.63$ . This strip is due to an enhancement of the number of stars of that colour, seen along the extent of the halo, caused by stars just prior and just after the turn off having the same colour. The leftmost edge of the strip ( $B-V \sim 0.5$ ), therefore, corresponds to the “spectral type” of the halo turn-off, around late F, as expected. However, a comparison with the data by Kron (1978) as reported by Bahcall & Soneira (1980) shows that in that case the mean colour is  $\sim 0.5$  and the edge of the strip is at about  $B-V = 0.4$ . Given the very large zenithal distance of Pavo as seen from La Silla, a zero point error of this magnitude cannot be ruled out (small variations in atmospheric extinction between observation of the field and of the standards could produce such an effect). If we “force” our data to agree with those of Kron, the resulting correlation of luminosity with colour would change from 0.065 to 0.056 mag( $B-V$ ) / Bmag. One should note also that if the error in zero point was indeed as large as to be able to destroy the correlation, the edge of the TO stars would move to  $B-V \sim 0.3$ , corresponding to an FO spectral type, clearly too early for the galactic halo turn off.

Moreover, the correlation over 6 magnitudes resulting in a total range in  $(B-V)$  of 0.38 (0.34) magnitudes does not appear to result from the passage of emission lines in the quasar spectra through the relevant filter band-passes as the result of varying redshift. Cristiani and Vio (1990) and Kinney, Rivolo and Koratkar (1990) have given quantitative measurements of the equivalent width of C IV 1550 as a function of absolute luminosities of quasars. Assuming that the Mg 2800 line luminosity scales in a similar manner, we have shown that the maximum blueing ( $z$  in the range 0.4–0.7) and the maximum reddening ( $z$  in the range 0.8–1.2) due to a luminosity range of 6 magnitudes is 0.06–0.11 in  $(B-V)$ , clearly less than the range discussed above.

The most natural and obvious explanation for this correlation lies in the fact that quasars (or AGN’s) reside in galaxies. As the intrinsic luminosity of the AGN becomes weaker, the redder colours of the galaxy have greater influence on the colours of the ensemble. This conclusion is reinforced by comparison with the sequence formed by AGN’s selected from the Véron and Véron Catalogue which includes resolved galaxies at the low luminosity end. The two sequences are similar and thus one might expect, with improved spatial resolution, to resolve in the first instance, the closer lower luminosity objects in the Pavo sample. We stress however that this result could be strengthened by the

accumulation of reliable photometry for a sample of quasars occupying small ranges in redshift  $z$  and a large range in intrinsic luminosity.

*Acknowledgements.* We are grateful to Frank Primini for making available the new reduction of the X-ray observations and acknowledge helpful correspondence and comments by him and Dan Harris. We are also grateful to Uli Zimmermann for providing reductions of our ROSAT Pavo data, the details of which will be published separately. Paolo Padovani assisted with the  $V/V_{max}$  test. Gianni Zamorani's careful critique of the paper has improved the presentation.

## References

- Bahcall, J.N., Soneira, R.M. 1980, *ApJ*, 238, L17
- Cristiani, S., Vio, R. 1990, *A&A*, 227, 385
- Cristiani, S., La Franca, F. 1995, in "Wide Field Spectroscopy and the Distant Universe", Proc. 35th Herstmonceux Conference, July 4–8 1994, S.J. Maddox and A. Aragon-Salamanca eds., World Scientific, Singapore - New Jersey - London - Hong Kong, p. 388
- Giacconi, R., et al. 1979, *ApJ*, 234, L1
- Giacconi, R., Zamorani, G. 1987, *ApJ*, 313, 20
- Gioia, I.M., Maccacaro, T., Schild, R.E., Wolter, A. 1990, *ApJS*, 72, 567
- Griffiths, R.E., Murray, S.S., Giacconi, R. et al. 1983, *ApJ*, 269, 375
- Griffiths, R.E., Tuohy, I.R., Brissenden, R.J.V., Ward, M.J. 1992, *MNRAS*, 255, 545
- Hasinger, G., Burg, R., Giacconi, R. et al. 1993, *A&A*, 275, 1
- Johnson, H.L. 1966, *ARA&A*, 4, 193
- Kinney, A.L., Rivolo, A.R., Koratkar, A.P. 1990, *ApJ*, 357, 338
- Kron, R.G. 1978, Ph.D. Thesis, University of California, Berkeley
- Oke, J.B. 1974, *ApJS*, 27, 21
- Primini, F.A., Murray, S.S., Huchra, J. et al. 1991, *ApJ*, 374, 440
- Setti, G. 1992, in "Frontiers of X-Ray Astronomy", ed. Y. Tanaka and K. Koyama (Universal Academy Press, Inc., and Yamada Science Foundation), p. 663
- Setti, G., Woltjer, L. 1982, in *Astrophysical Cosmology, Proc. Vatican Study Week on Cosmology & Fundamental Physics*, ed. H.A. Bruck, G.V. Coyne, and M.S. Longair (Vatican City: Pontificia Academia Scientiarum), p. 315
- Véron-Cetty, M.-P., Véron, P. 1996, Scientific Report No. 17, European Southern Observatory
- Wilkes, B.J., Tananbaum, H., Worrall, D.M. et al. 1994, *ApJS*, 92, 53
- Zitelli, V., Mignoli, M., Zamorani, G., Marano, B., Boyle, B.J. 1992, *MNRAS*, 256, 349